GNSS and HF radar measurements for detecting F-region irregularities in the Taiwan-Philippines sector

Prof. Dr. Lung-Chih Tsai[1,2]

1) Center for Space and Remote Sensing Research, National Central University (NCU), Taiwan
2) GPS Application and Research Center, NCU, Taiwan

Ref 1: Tsai, L.-C., S.-Y. Su, J.-X. Lv, T. Bullett, and C.-H. Liu (2022), Multi-station and multi-instrument observations of F-region irregularities in the Taiwan-Philippines sector, *Remote Sens.*, 14, 2293, https://doi.org/10.3390/rs14102293

Ref 2: Tsai, L.-C., S.-Y. Su, C.-H. Liu, H. Schuh, J. Wickert, and M. M. Alizadeh (2021), Diagnostics of Es layer scintillation observations using FS3/COSMIC data: Dependence on sampling spatial scale, *Remote Sens.*, 13, 3732, https://doi.org/10.3390/rs13183732

Contents:

- Introduction
- System Description: FS7/COSMIC2, ground-based GPS receiver, software-defined GPS receiver, & VIPIR (HF radar)
- Scintillation index S4 determination: dependence on sampling spatial scale / sampling rate
- Results: scintillation & ESF specifications in the Taiwan-Philippine sector
- Discussions & Conclusions

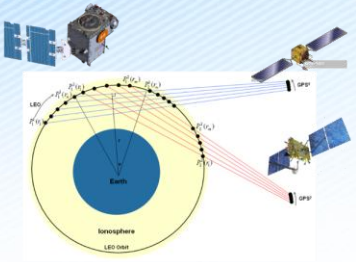

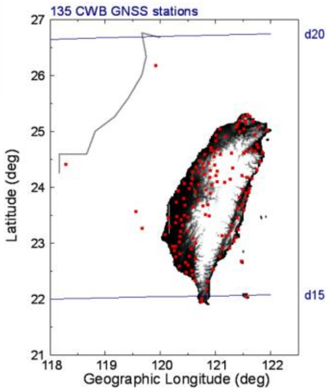

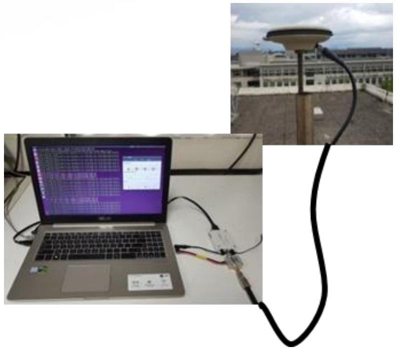

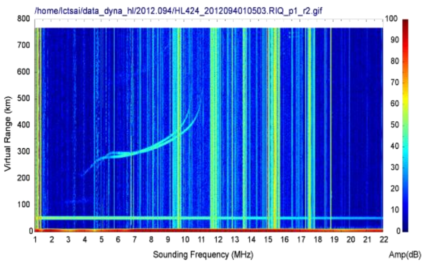

FormoSat7/COSMIC2 radio occultation (RO) observations

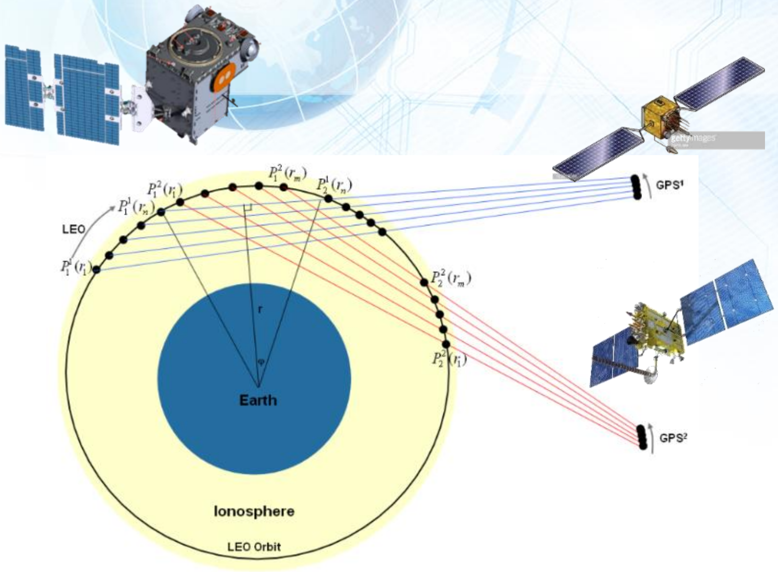

	First Phase Launch (no 2nd phase mission)
Mission Constellation	***6 satellites (low inclination 24 deg, mission altitude ~550 km, & separation 60 deg)***
Mission Payload	***GPS & Glonass Rx***
Science Payload	***•2-band beacon •plasma drift/fluctuation sensor (~10kg, 22W)***
Launch Schedule	***June 25, 2019***
Mission Duration	***10 years***

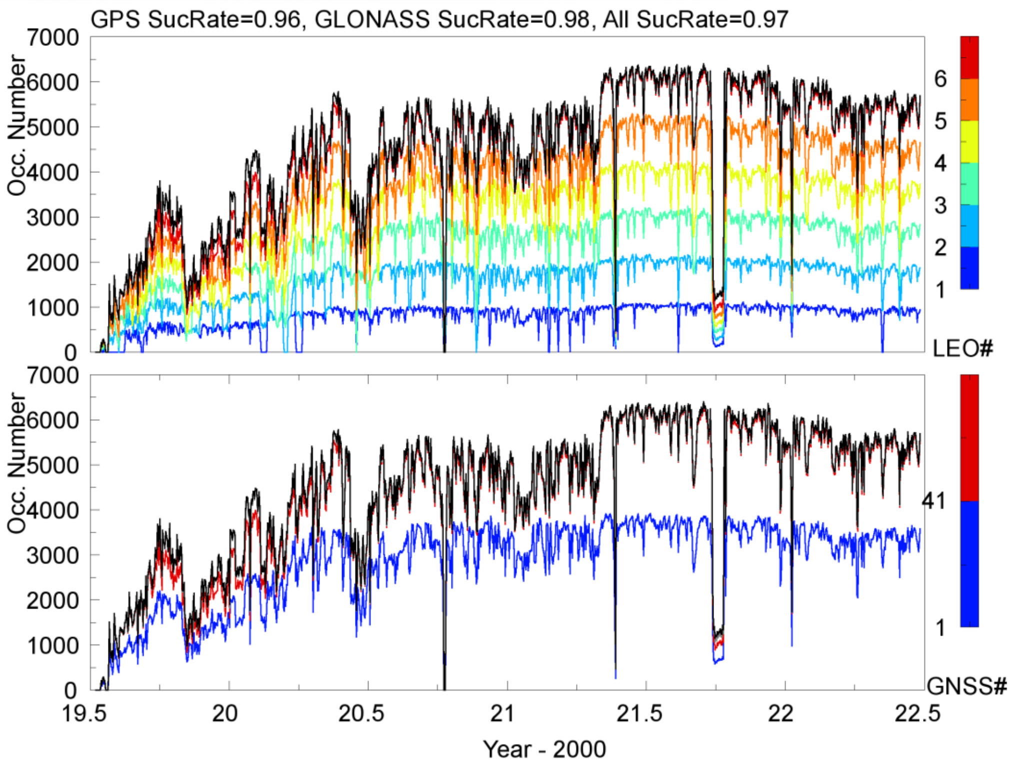

Yearly global occurrence distributions of scint. events (undersampling 1-Hz S4L1max > 0.1) in FS7/COSMIC2

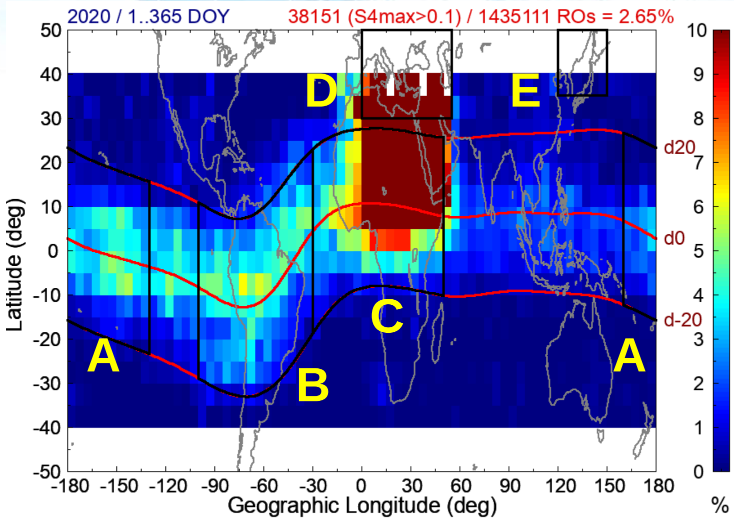

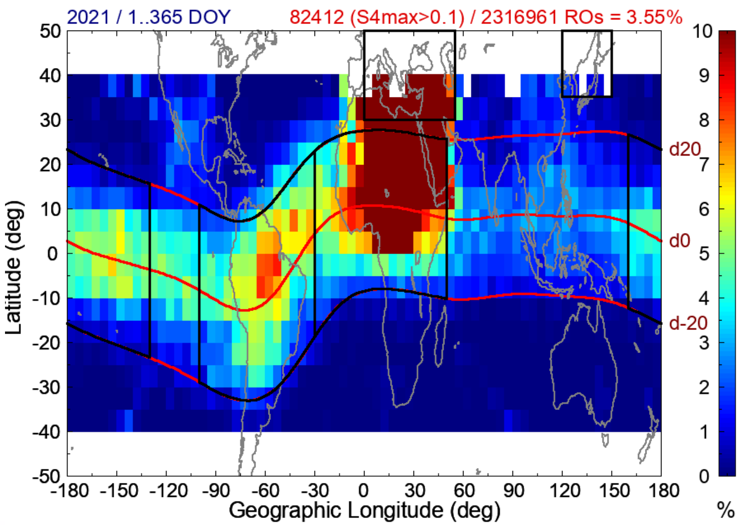

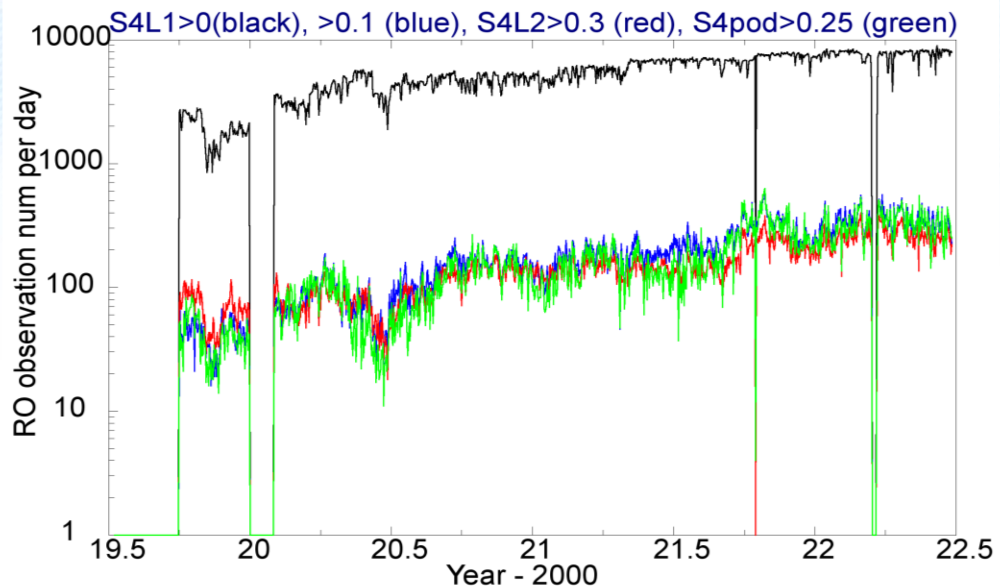

The numbers of RO observations (in black) and scint. events (blue & red: 1-Hz S4L1 & S4L2 data, green: on-board 50-Hz data)

Five identified scintillation areas are :

A. Central Pacific Area: -20°~20° dip latitude, 160° E~130° W
B. South American Area: -20°~20° dip latitude, 100° W~30° W
C. African Area: -20° ~20° dip latitude, 30° W~50° E
D. European Area: 30° ~55° N, 0° ~55° E;
E. Japan Sea Area: 35°~55° N, 120° ~150° E

Yearly global occurrence distributions of scint. events (onboard 50-Hz S4L1max > 0.25) in FS7/COSMIC2

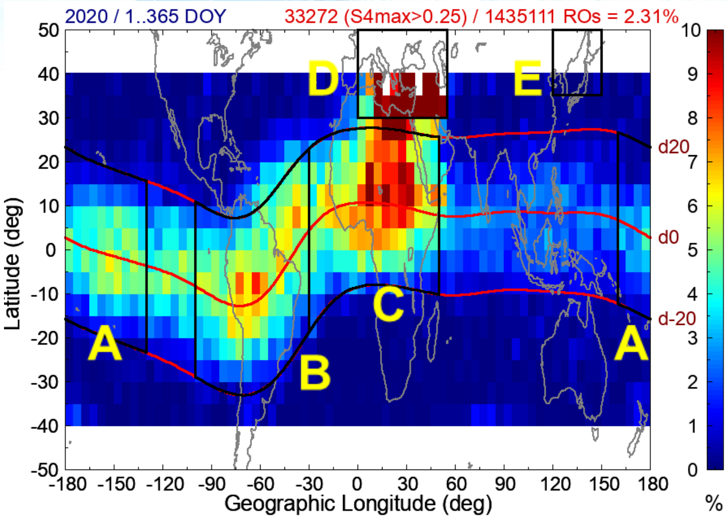

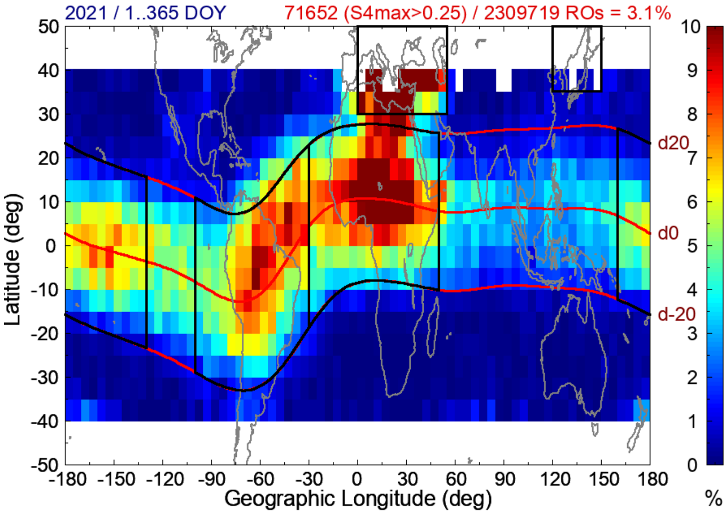

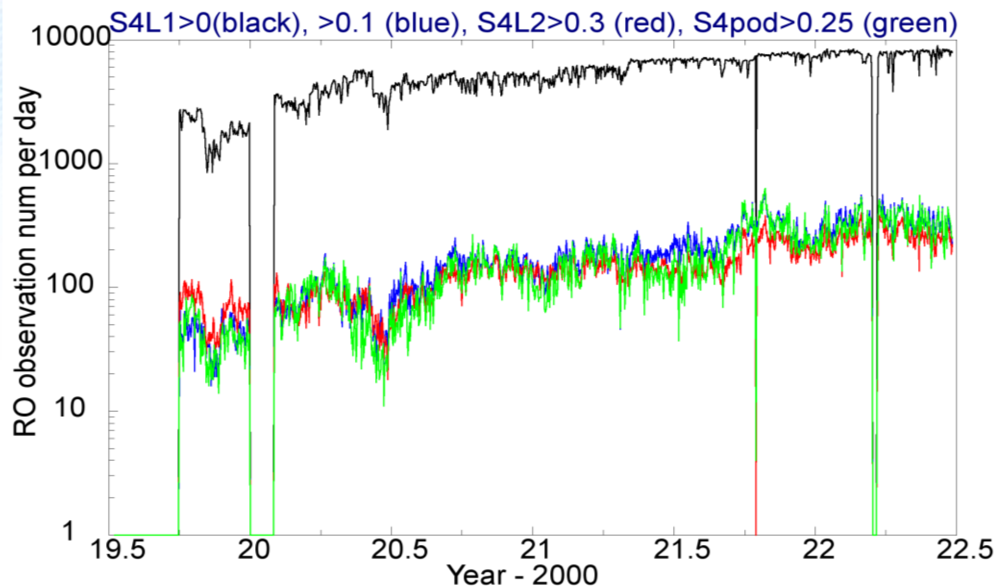

The numbers of RO observations (in black) and scint. events (blue & red: 1-Hz S4L1 & S4L2 data, green: on-board 50-Hz data)

Five identified scintillation areas are :

A. Central Pacific Area: -20°~20° dip latitude, 160° E~130° W

B. South American Area: -20°~20° dip latitude, 100° W~30° W

C. African Area: -20° ~20° dip latitude, 30° W~50° E

D. European Area: 30° ~55° N, 0° ~55° E;

E. Japan Sea Area: 35°~55° N, 120° ~150° E

GNSS RO scintillation observation: Limb-viewing SNR, undersampling S4, & N_e profiles from FS7/COSMIC2 GPS/GLONASS RO ob. On Oct. 26, 2021

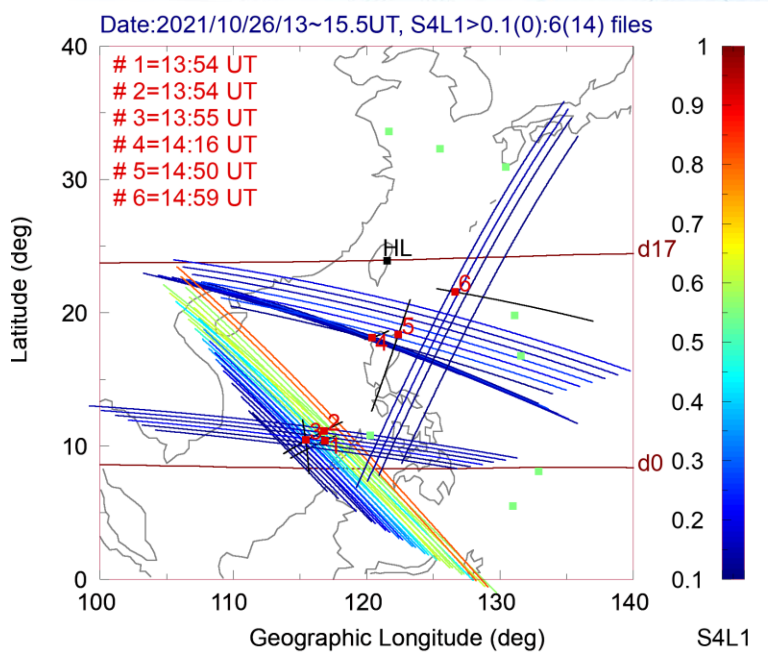

$$N_e(r_t) = N_e(r_{top}) - \frac{1}{\pi}\int_{r_t}^{r_{top}} \frac{d\,TEC'(r)/d\,r}{\sqrt{r^2 - r_t^2}}\,d\,r$$

$$S4L1\,(or\ S4L2) = \frac{\sqrt{\langle A^4\rangle - \langle A^2\rangle^2}}{\langle A^2\rangle}$$

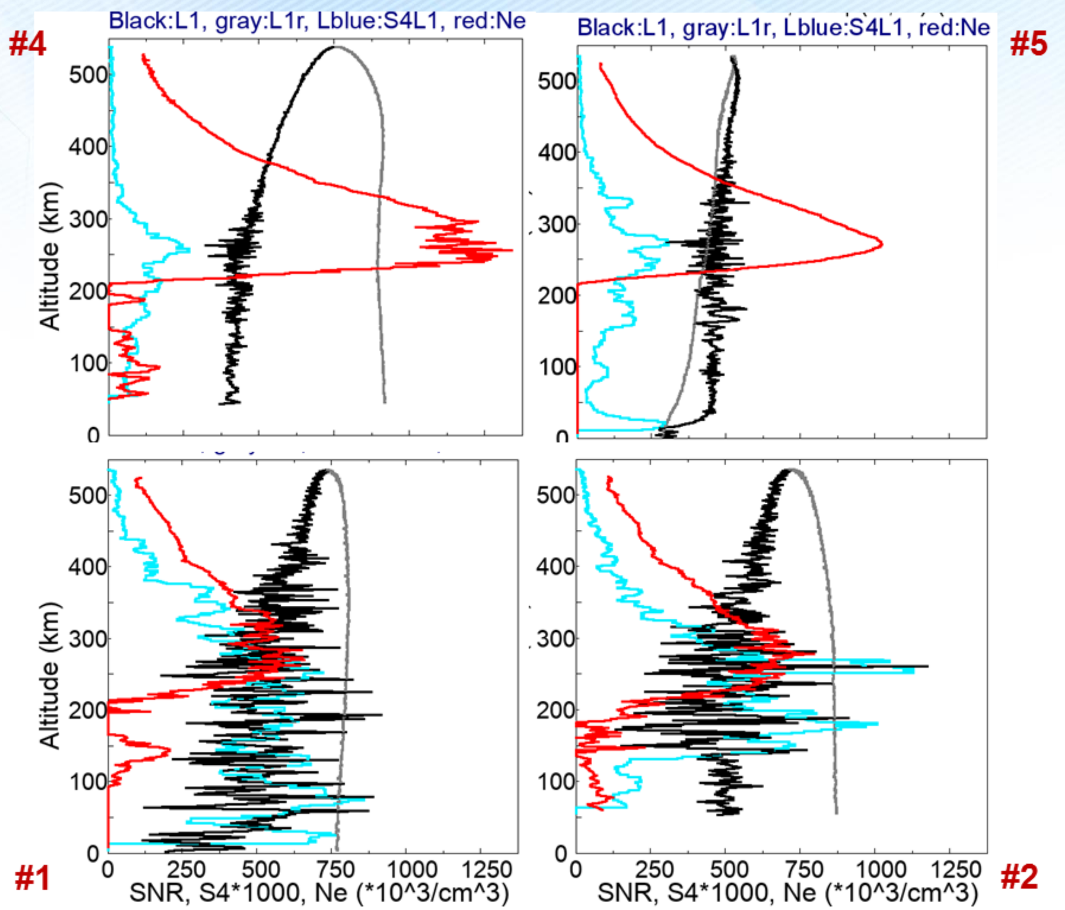

Note: The irregularities at higher latitudes should be the latitudinal mapping-out facts from lower latitudes.

Scintillation index S4 determination:
dependence on sampling spatial scale / sampling rate

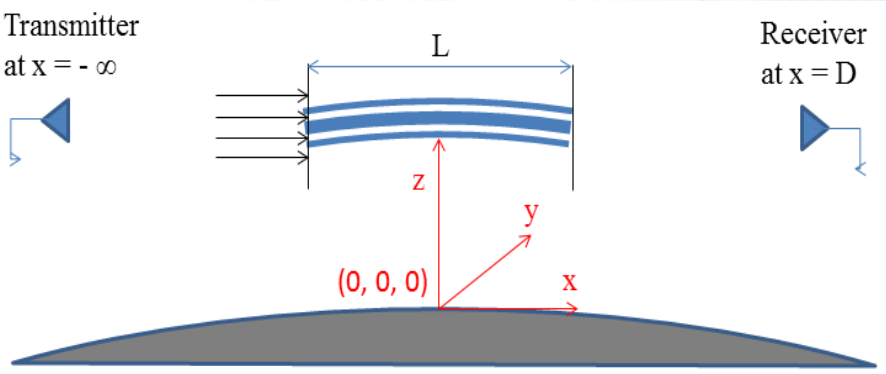

A parabolic wave equation for field

$E = u(x, \rho_t)\, exp(-ikx)$

$$-2jk\frac{\partial u}{\partial x} + \nabla_t^2 u = -k^2 \varepsilon_1(x,\rho_t)u,$$

$$where\ -L/2 < x < L/2,\ and\ \nabla_t^2 = \frac{\partial^2}{\partial y^2} + \frac{\partial^2}{\partial z^2}.$$

$$-2jk\frac{\partial u}{\partial x} + \nabla_t^2 u = 0, \quad where\ x > L/2.$$

The fluctuating part of dielectric permittivity and a power-law irregularity spectrum:

$$\varepsilon_1(x,\rho_t) = -\frac{\left(f_{p0}/f\right)^2\left[\Delta N(x,\rho_t)/N_0\right]}{1-\left(f_{p0}/f\right)^2} \approx -\frac{e^2}{4\pi^2\varepsilon_0 m f^2}\Delta N(x,\rho_t).$$

$$\Phi_{\Delta N}(\kappa) = \frac{\sigma_N^2\,\Gamma\left(\frac{p}{2}\right)\kappa_0^{p-3}}{\pi^{3/2}\,\Gamma\left(\frac{p-3}{2}\right)}\left(\kappa^2+\kappa_0^2\right)^{-p/2} \propto \kappa^{-p},\ where\ p\ is\ spatial\ index.$$

Scintillation index S4 determination using the Ryton approximation

$$u(x,\rho_t) = u_0 \exp[\psi(x,\rho_t)] = u_0 \exp[\chi(x,\rho_t) - jS_1(x,\rho_t)],$$

$$\Phi_\chi(0,\kappa_t) = \frac{\pi k^2 L}{4}\left[1 - \frac{2k}{\kappa_t^2 L}\sin\left(\frac{\kappa_t^2 L}{2k}\right)\cos\left(\frac{\kappa_t^2 (x - L/2)}{k}\right)\right]\Phi_{\varepsilon_1}(0,\kappa_t).$$

$$\left\langle \chi^2 \right\rangle = B_\chi(0) = \iint \Phi_\chi(0,\kappa_t) d^2\kappa_t$$

$$= \frac{\sigma_N^2 \Gamma\left(\frac{p}{2}\right) L}{2^{\frac{p}{2}} \pi^{\frac{p+1}{2}} \Gamma\left(\frac{p-3}{2}\right)} \times$$

$$\iint \left[1 - \frac{1}{\pi}\frac{\kappa_F^2}{\kappa_t^2}\frac{x}{L}\sin\left(\pi\frac{\kappa_t^2}{\kappa_F^2}\frac{L}{x}\right)\cos\left(2\pi\frac{\kappa_t^2}{\kappa_F^2}\frac{\left(x - \frac{L}{2}\right)}{x}\right)\right]\frac{\kappa_0^{p-3} k^{2-p/2} x^{p/2}}{\left(\frac{\kappa_t^2}{\kappa_F^2} + \frac{\kappa_0^2}{\kappa_F^2}\right)^{p/2}} d^2\kappa_t,$$

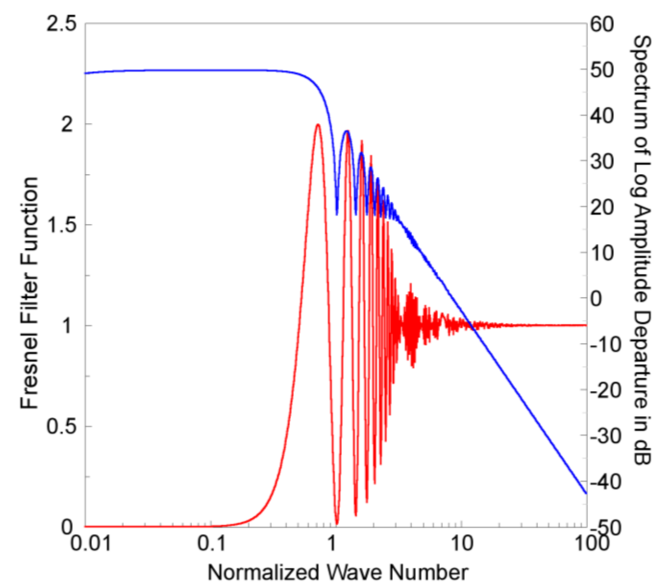

Fresnel filter function in red and Φχ() in blue

The scintillation index S4: $S_4^2 = \frac{\left\langle \left(I - \langle I \rangle\right)^2 \right\rangle}{\langle I \rangle^2} \approx \frac{4\left\langle \chi^2 \right\rangle + 24\left\langle \chi^2 \right\rangle^2}{1 + 4\left\langle \chi^2 \right\rangle + 8\left\langle \chi^2 \right\rangle^2}$. $S_4^2 \approx 4\left\langle \chi^2 \right\rangle$ *for small S4.*

The normalized amp standard deviation S2: $S_2^2 = \frac{\left\langle \left(u_a - \langle u_a \rangle\right)^2 \right\rangle}{\langle u_a \rangle^2} = \frac{\left\langle u_0^2 \exp(2\chi) \right\rangle}{\left\langle u_0 \exp(\chi) \right\rangle^2} - 1 \approx \frac{\left\langle \chi^2 \right\rangle + \frac{3}{2}\left\langle \chi^2 \right\rangle^2}{1 + \left\langle \chi^2 \right\rangle + \frac{1}{2}\left\langle \chi^2 \right\rangle^2} \sim \left\langle \chi^2 \right\rangle$ *for small S4.*

Scintillation index S4 determination: complete ($\kappa_t > \kappa_F$, i.e. $f_s > f_F$) or underestimated ($\kappa_t < \kappa_F$, i.e. $f_s < f_F$)

Theoretic simulations on S4 and S2 v.s. normalized wave number (κ_t / κ_F), and the wave number of FFZ: $\kappa_F = 2\pi/D_F$

$$Note: \quad \langle \chi^2 \rangle = \iint \Phi_\chi(0, \kappa_t) d^2\kappa_t$$

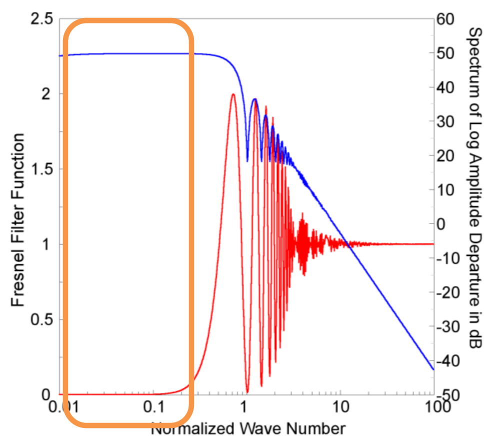

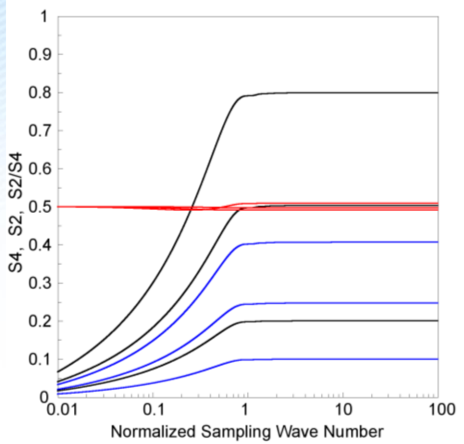

Experimental results from FS3/COSMIC Es observations on S4 (in black) and S2 (in red) v.s. κ_t / κ_F

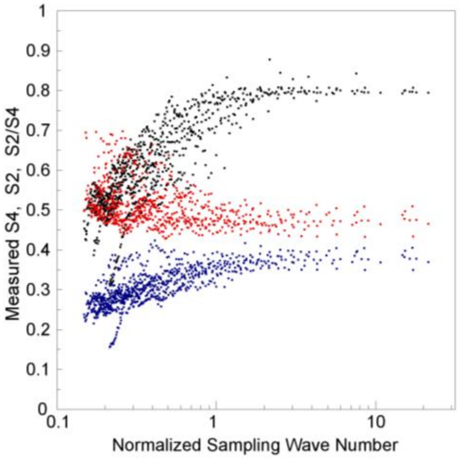

Complete S4~0.8

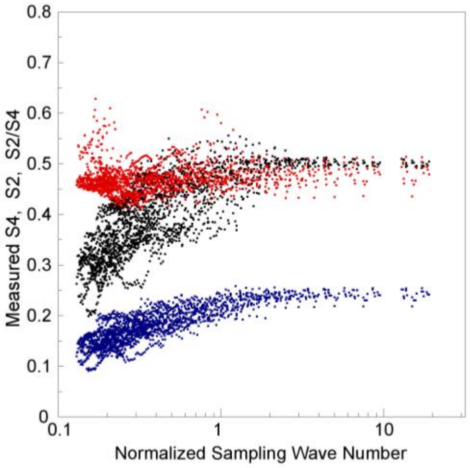

Complete S4~0.5

135 ground-based GPS receivers (left panel) from the CWB, Taiwan, and software-defined GPS receivers (right panel, green labels)

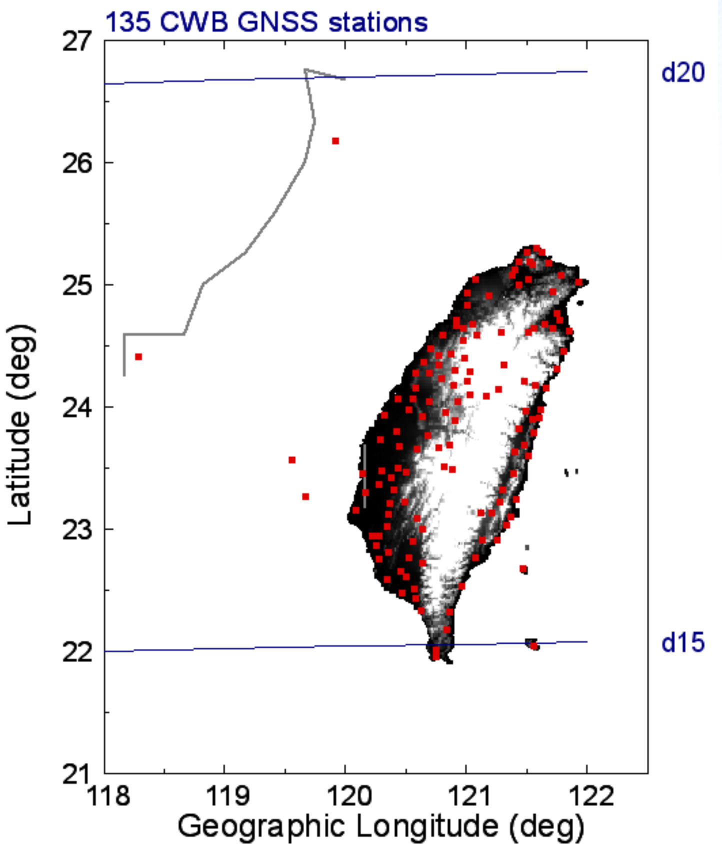

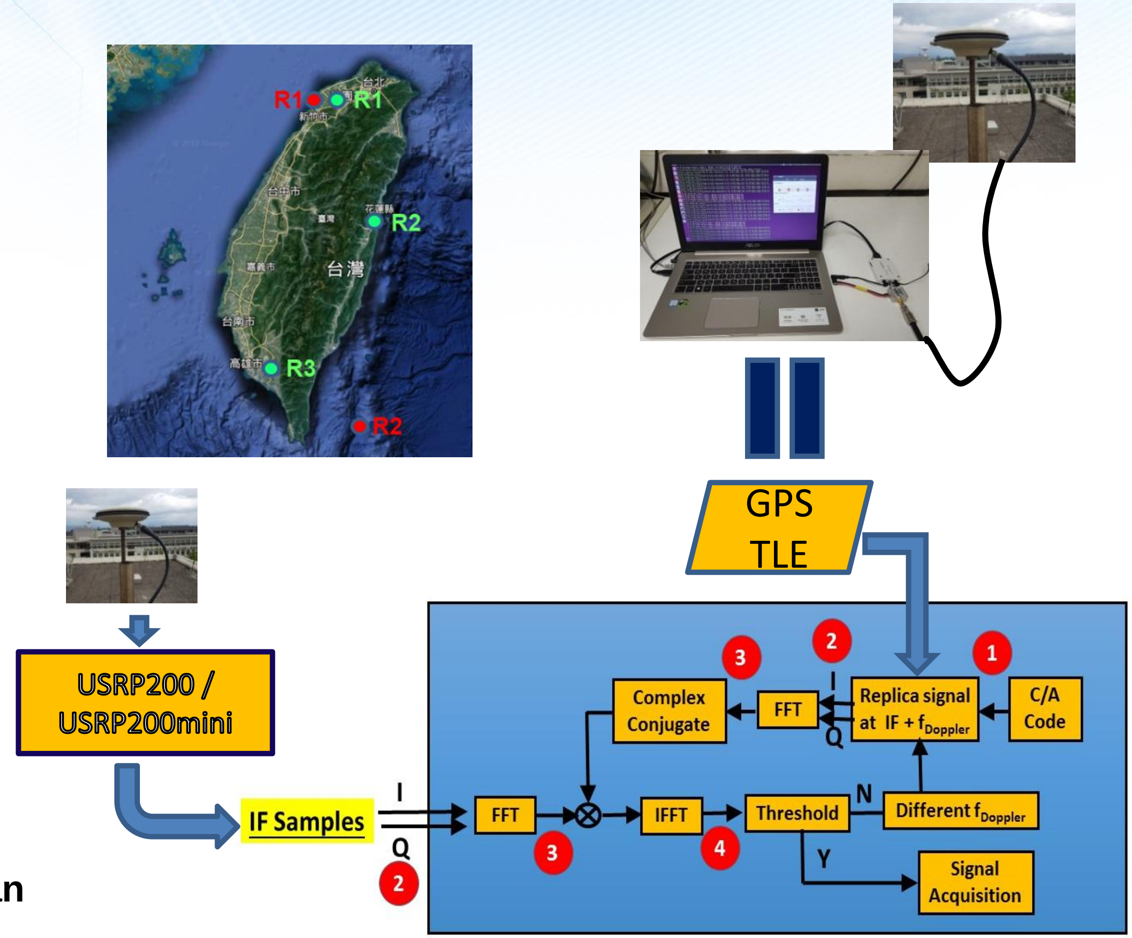

CWB: Central Weather Bureau of Taiwan

Two-dimensional scintillation index VS_4 maps (v_E>0) derived by the CWB GPS data (133 Rxs & 1-Hz) on Oct. 26,

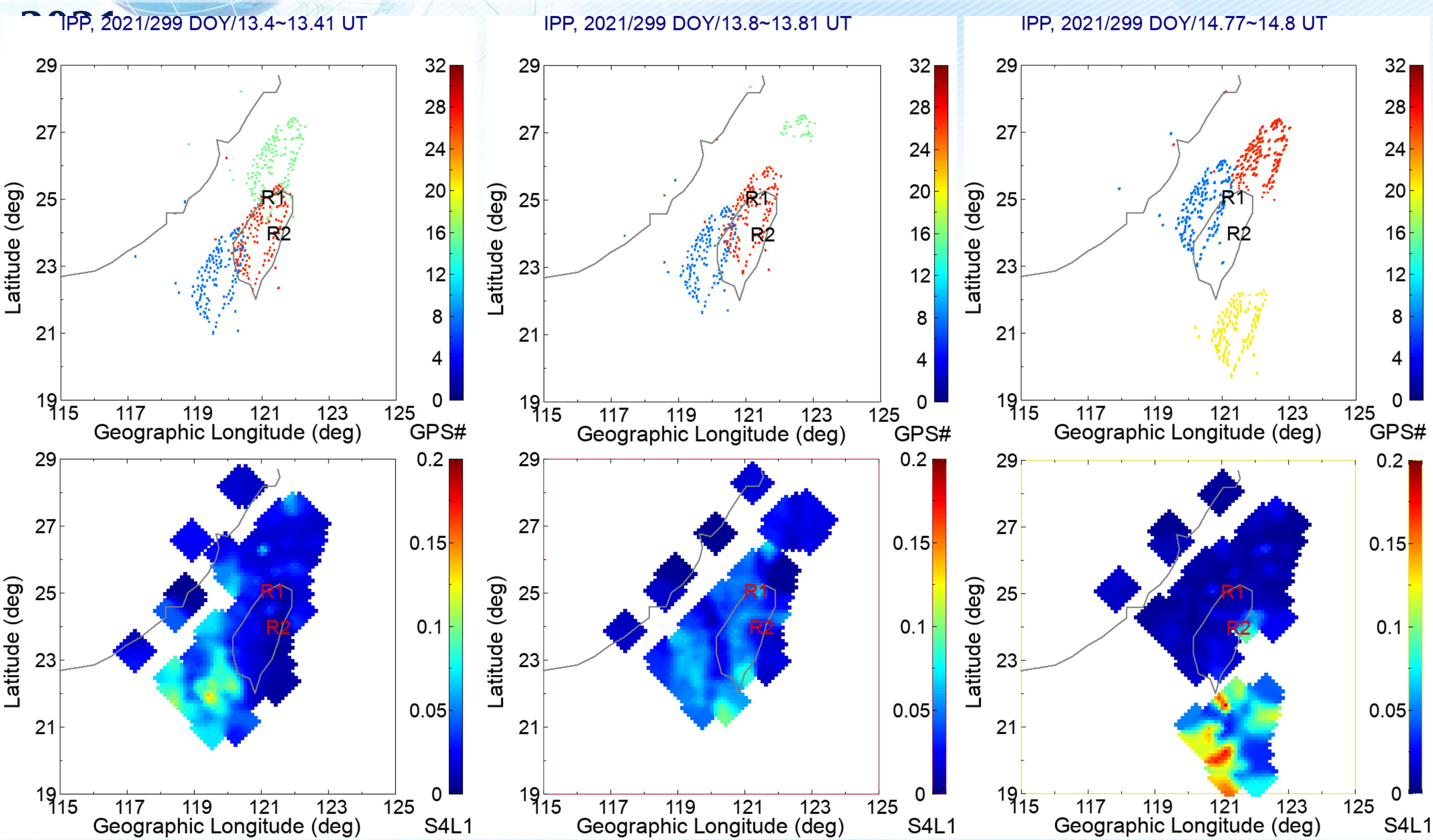

Spectrum analyses of GPS #27 (upper), #8 (middle), & #21 (bottom) signals from the Chungli software-defined GPS receiver

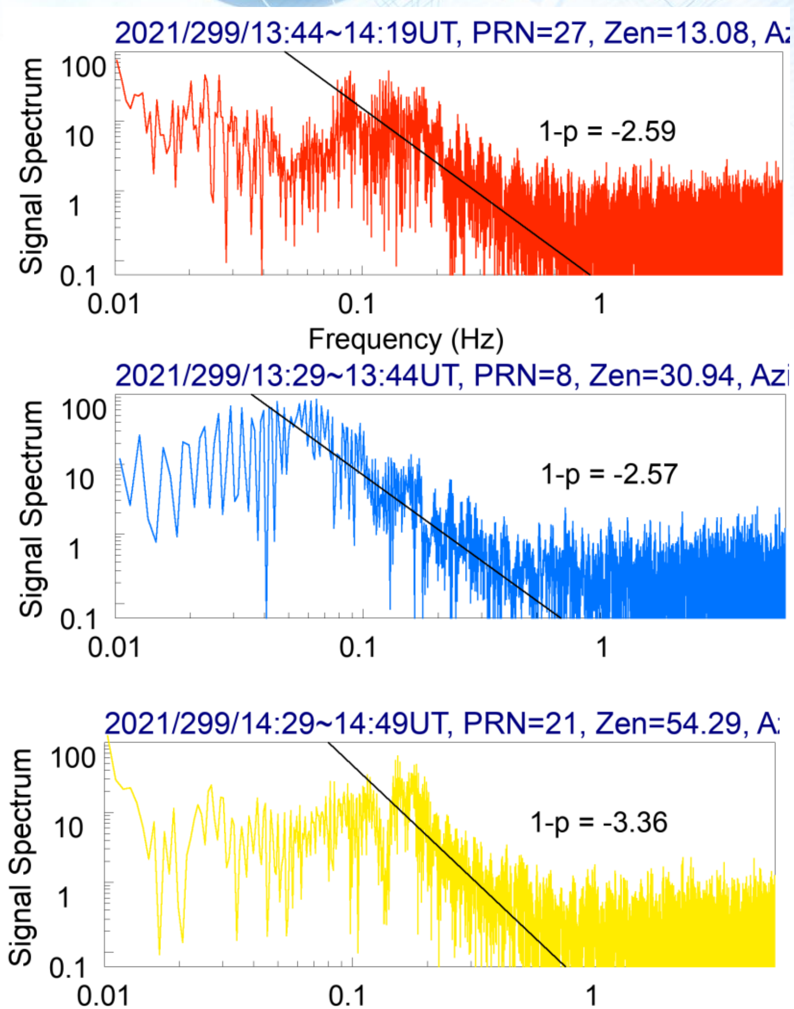

$$\text{the Fresnel freq } f_F = \frac{v}{\sqrt{2\,\lambda\,L}}$$

	p	f_B (breaking f)	f_F (v_I=0)	v_N
GPS#27	3.59	0.1 Hz	~0.2 Hz	>0
GPS#8	3.57	0.07 Hz	~0.2 Hz	>0
GPS#21	4.36	0.15 Hz	~0.2 Hz	>0

Note: the targeted plasma irregularities moved eastward and northward, and smaller irregularity scale higher the spectral index and stronger scintillation intensity.

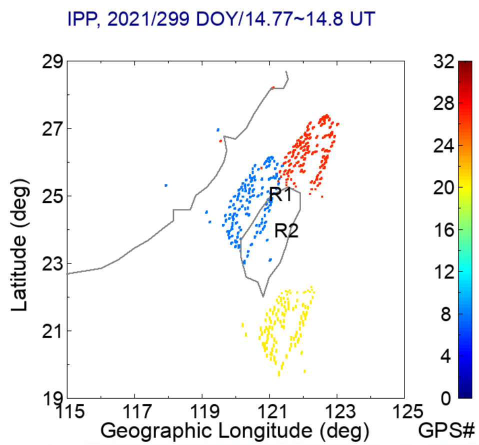

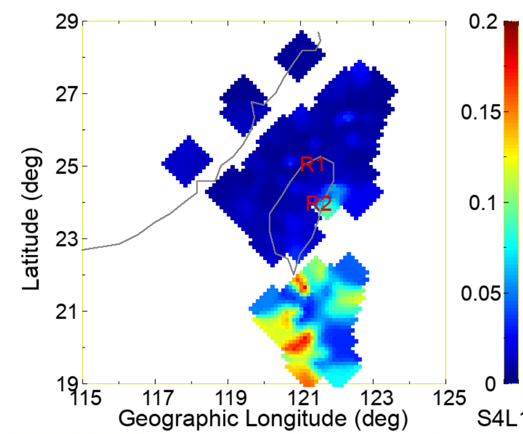

HF radar observations:

the Hualien and Lonquan Vertical Incidence Pulsed Ionospheric Radars (VIPIRs) in Taiwan

Ionogram

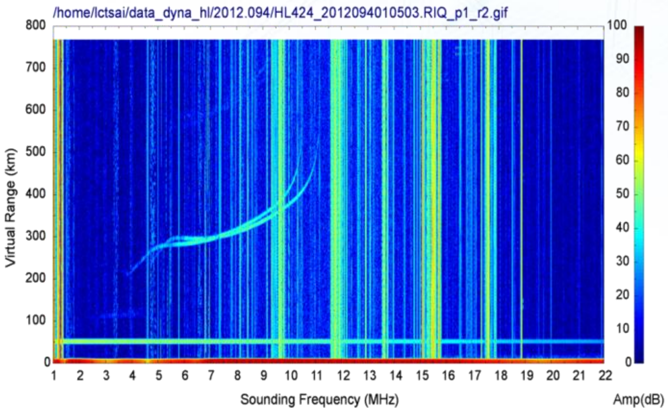

MF/HF RF surveillance

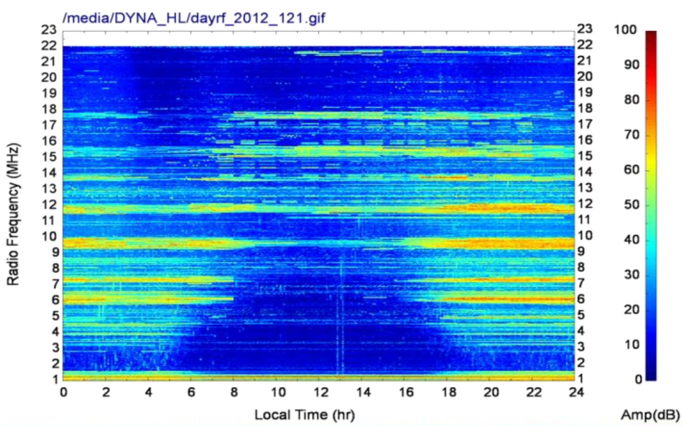

Ionosphere

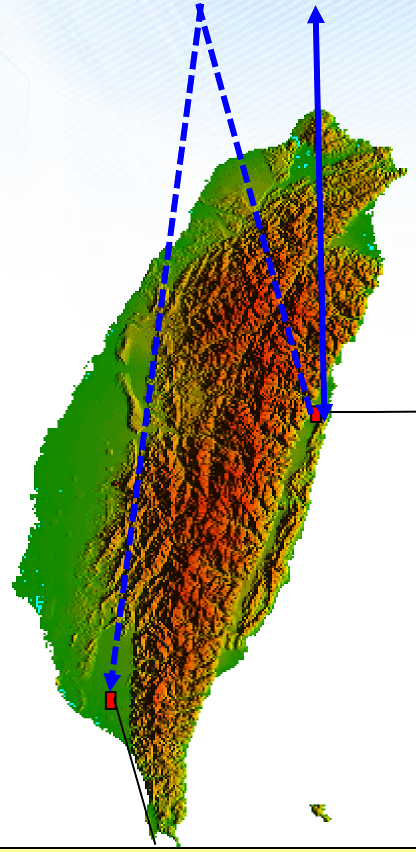

Hualien
(23.89 ° N ,121.55 ° E)

Longquan
(22.67° N, 120.60° E)

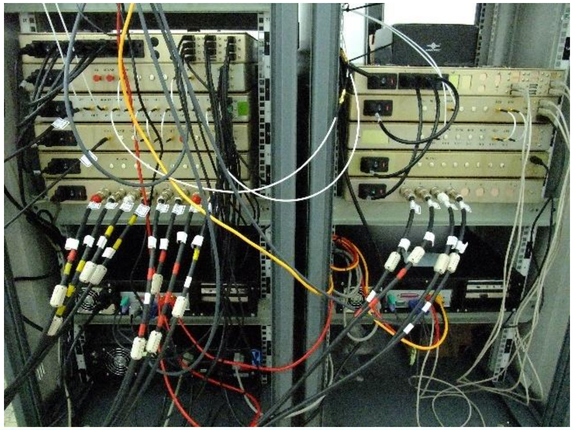

ESF ionograms recorded by the Hualien VIPIR on Oct. 26, 2021

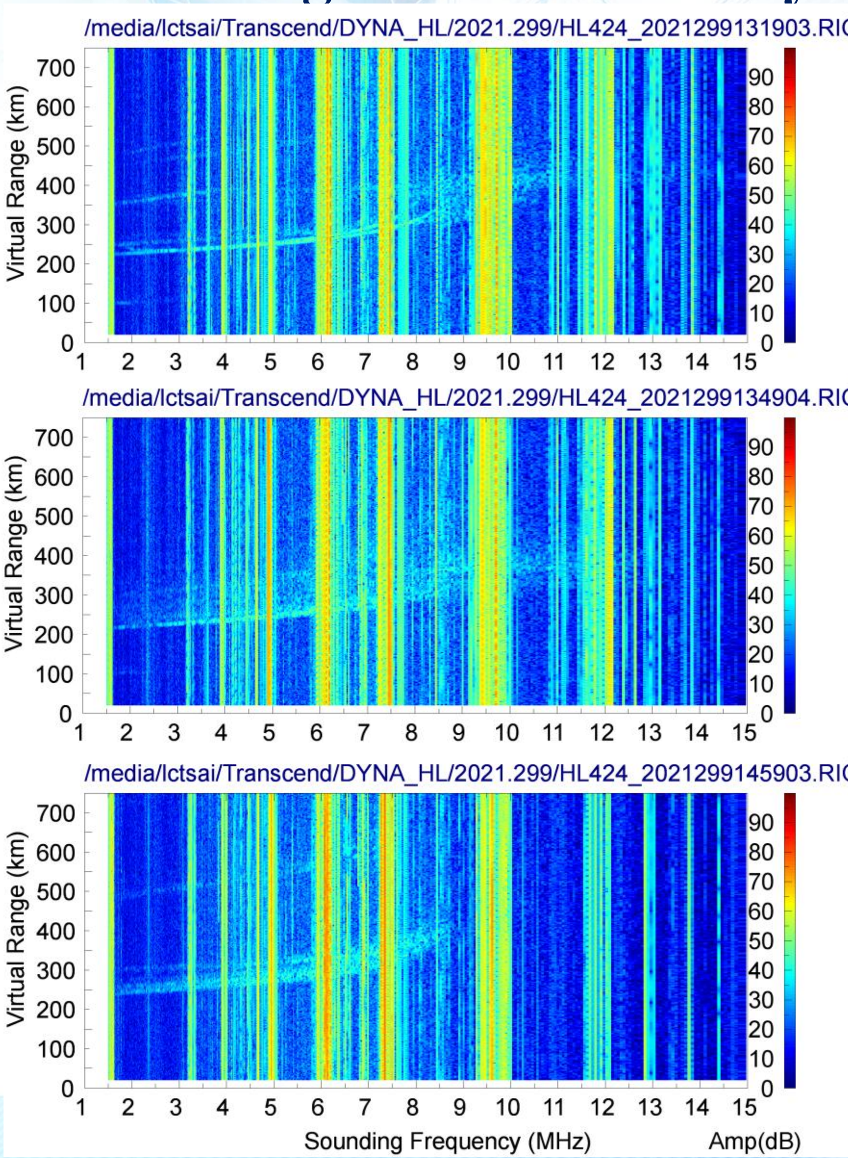

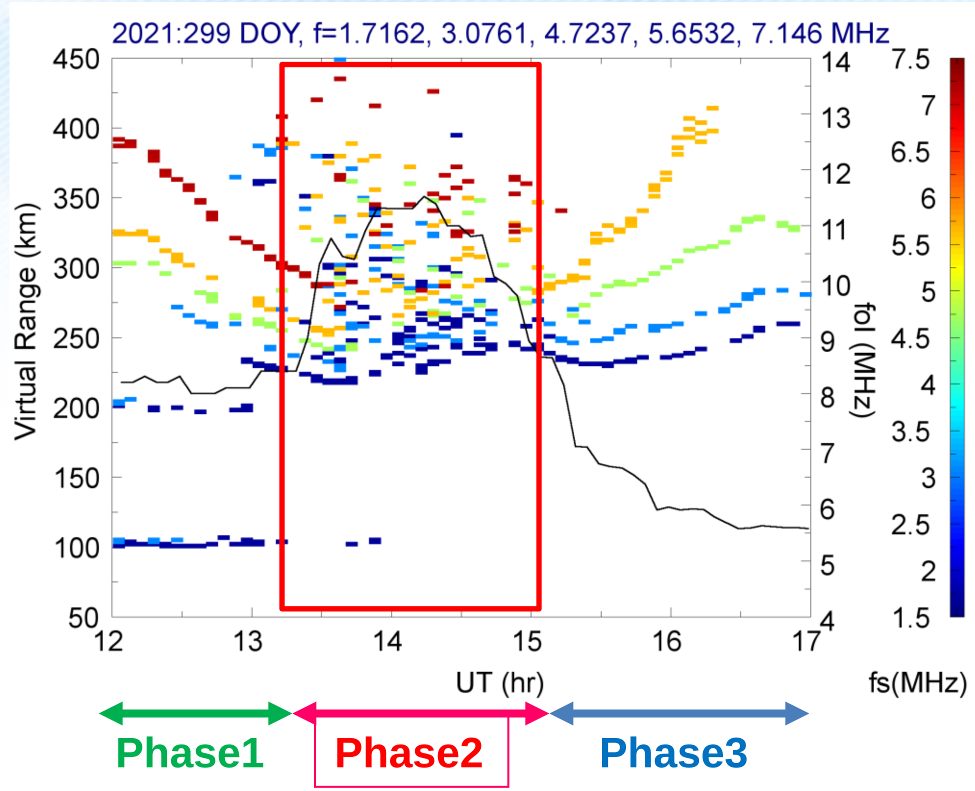

Phase 1: similar *foF2, h'F* ↓ => PRE phase

Phase 2: spread features => ESF phase

Phase 3: *foF2* ↓, *h'F* ↑ => nighttime ionosphere

Conclusions and Final Remarks

- Fresnel frequency is an important parameter for scintillation index S4 or S2 determination to be complete or underestimated.
- A multi-station and multi-instrument system, organized and proposed for ionospheric scintillation and equatorial spread-F (ESF) specification and their associated motions in the Taiwan-Philippines sector, is ready.
- The irregularities (observed on Oct. 26, 2021) at higher latitudes should be the latitudinal mapping-out facts from lower latitudes, and there are stronger irregularities around F-layer peak because of greater conductivities.
- The targeted plasma irregularities (observed on Oct. 26, 2021) moved eastward and northward, and smaller irregularity scale higher the spectral index and stronger scintillation intensity.
- A post sunset decrement on the virtual heights of fixed-frequency ionospheric echoes could be good precursors for post sunset scintillation and ESF events caused by pre-reverse enhanced (PRE) field.

Future works:
the east-Asia VIPIR network

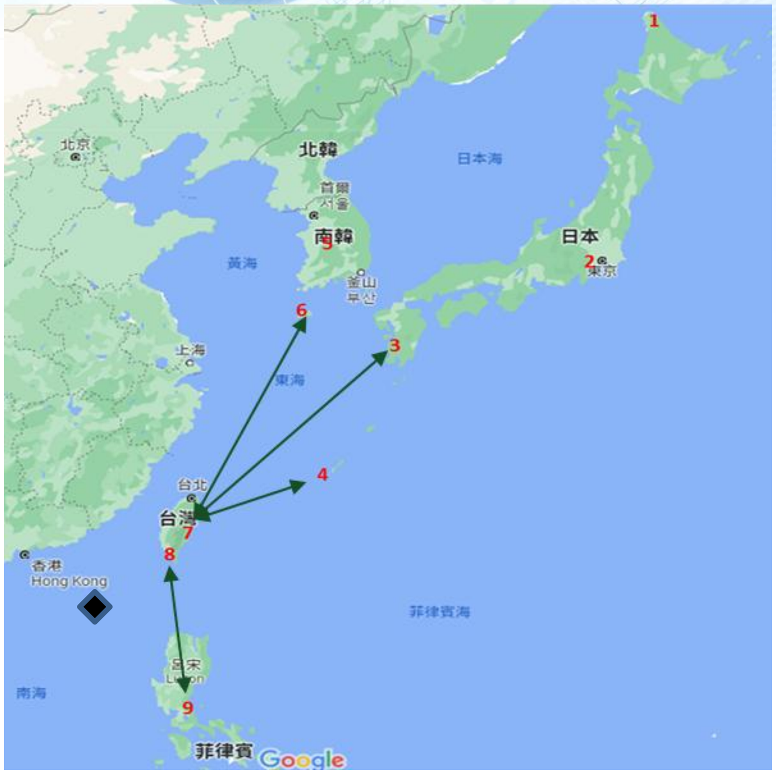

Cooperations:

NCU/Taiwan, KSWC/Korea, NICT/Japan, NOAA/NCEI/CIRES/USA

VIPIR sites：

1. Wakkanai/Sarobetsu (45.16 ° N , 141.75 ° E)，
2. Kokubunji (35.71° N , 139.49° E)，
3. Yamagawa (31.20° N , 130.62° E)，
4. Okinawa/Ogimi (26.68° N , 128.15° E)，5. Geosan (36.77° N , 127.82° E)，
6. Jeju (33.50° N , 126.53° E)，
7. Hualien (23.89° N , 121.55° E)，
8. Longquan (22.67° N , 120.60° E)，and
9. Malina(14.61° N , 120.96°

Potential site：

♦ Pratas island (20.7 ° N , 116.71 ° E)

Working/studying topics:
Oblique sounding observations, regional ionospheric N_e or parameter map, ionospheric irregularity and scintillation prediction, ray tracing and/or wave propagation analyses.

Thanks for your attention !